Proceedings of Ninth World Conference on Earthquake Engineering
August 2-9, 1988, Tokyo-Kyoto, JAPAN (Vol.VIII)

SI-R1

State-of-the Art Report
RECENT DEVELOPMENT ON DYNAMIC MODEL TESTING IN GEOTECHNICAL ENGINEERING

Andrew N SCHOFIELD and R Scott STEEDMAN

Cambridge University Engineering Department,
Trumpington Street, Cambridge, UK

SUMMARY

The main item of equipment for experimental study of geotechnical models in earthquakes is the shaking table. Recently it has become possible to test geotechnical models in shaking tables during centrifuge flight. This paper gives a brief introduction to the principles of modelling and some experimental details of the facilities. Typical models are described and the behaviour of soil in different tests is discussed. It is concluded that the recent centrifuge developments will lead to studies on normal shaking tables being organised in conjunction with centrifugal model tests.

SHAKING TABLES MOUNTED IN GEOTECHNICAL CENTRIFUGES

The soil embankment shown in plane section in Fig. 1 rests on a horizontal foundation. The soil pores are saturated with pore fluid and an impermeable mass rests on the embankment crest. The lowest trace in Fig. 2 shows a horizontal motion of the foundation which is approximately sinusoidal for ten equal cycles: the central trace shows that the motion of the mass is at first in phase with the foundation, with some amplification of the motion between the foundation and the embankment crest. Half way through the shaking there is a phase shift and a reduction of the motion of the mass, indicating that there has been a loss of stiffness of the embankment.

The trace for pore pressure transducer PPT68 in Fig. 2 shows the pore fluid pressure at the centre of the crest, below the impermeable mass. At first there is a cyclic increase in pore pressure, but half way through the shaking the pressure reaches and remains at a plateau. At that stage incompressible pore fluid is supporting the weight that rests on the embankment crest. The pore pressure increase has led to a fall in the effective stress that rests on the interlocking aggregate of soil particles. The fall in effective stress has led to the reduction in stiffness in the embankment and to the inertial effects that are evident in Fig. 2. These test data come from a shaking table mounted in a geotechnical centrifuge (Ref. 1) and they serve as an introduction to the discussion of this recent development of earthquake model tests.

Consider a point within a full scale prototype embankment, at which the displacements, velocities and accelerations are

$$x = a \sin \omega t$$

$$dx/dt = a\omega \cos \omega t \qquad (1)$$

$$d^2x/dt^2 = -a\omega^2 \sin \omega t$$

If the embankment is modelled at 1/N scale on a normal shaking table in earth's gravity the frequency is increased by a factor of $\sqrt{N}$, so that displacements, velocities and accelerations at the homologous point in the model become

$$x = a/_N \sin \sqrt{N}\omega t$$

$$dx/dt = a\omega/_{\sqrt{N}} \cos \sqrt{N}\omega t \qquad (2)$$

$$d^2x/dt^2 = -a\omega^2 \sin \sqrt{N}\omega t$$

If the problem involved only the ratio of inertial force and weight, $a\omega^2/g$ (where g is the acceleration of earth's gravity), then that model might correctly represent the prototype. However the magnitude of stress has a strong effect on the behaviour of an interlocking aggregate of soil particles. Stress magnitudes can be reproduced if a model is subjected to a steady acceleration Ng in a centrifuge, and then shaken with a frequency increased by a factor N. The displacements, velocities and accelerations are then given by

$$x = a/_N \sin N\omega t$$

$$dx/dt = a\omega \cos N\omega t \qquad (3)$$

$$d^2x/dt^2 = -Na\omega^2 \sin N\omega t$$

The ratio of inertial force and weight $Na\omega^2/Ng = a\omega^2/g$ is correct, and so also are the stress magnitudes: the integral of (depth to the point) x (density of soil above the point) x (acceleration) causes the same weight to rest on the soil in the model that occurs at the point in the prototype because in the centrifuge model and the prototype the product of (length x acceleration) are identical.

There has been a rapid increase in the number of papers on geotechnical centrifuge operations published recently (Refs. 2,3,4) and now several organisations that are operating normal shaking tables are interested in making tests on shaking tables mounted in geotechnical centrifuges. At a time of many developments it is not appropriate in this brief paper to dwell on features of early work that have already been overtaken, but there are some simple points that are worth noting. For example, Fig. 3 shows the equipotential surface of centrifugal acceleration to be a paraboloid of revolution about the centrifuge axis. In the Cambridge 4 m radius centrifuge, on which the data of Fig. 2 were obtained, the embankment model I lay in the plane of rotation of the centrifuge. The radial acceleration field departs from the normal to the base of the model. The shaking motion lies within the plane of rotation and therefore Coriolis accelerations also cause errors. In contrast, on the 5.5 m radius LCPC centrifuge at Nantes a plane embankment model II is placed perpendicular to the plane of rotation of the centrifuge, and this reduces the departure of the acceleration field from the normal to the base of the model and the Coriolis accelerations during base shaking.

The scale factor for volume and mass in a centrifuge is N^3, and the LCPC centrifuge can test a payload of 500 kg at a scale N = 200, which is equivalent to 500 x 200^3 kg = 4000 million tonnes in a prototype. In a static model test perhaps half of the payload mass is soil and half is the strong rigid container forming the plane walls which contain the plane faces of the model. In dynamic

tests part of the payload is used up by the dynamic actuator. The early actuators have involved release of springs or hammers, firing of explosives, excitation of piezoelectric crystals, discharge of oil at high pressure through an electro hydraulic valve and so on. The shaking mass can be reduced if the model rests on a sliding plate within a container, so that only the model and the plate require excitation and not the whole container. This concept is attractive because the force and power required to drive a shaker are both directly proportional to the mass. Table 1 gives values for the peak power required for shakers to generate a 20% earthquake at 50Hz in a 100g centrifugal model flight.

Table 1

shaking mass (kg)	50	300	1000
force (kN)	10	60	200
power (kW)	3	19	63

Careful consideration must be given to the design of shakers for large geotechnical centrifuges as some early low-power actuator systems have features which will prevent their future development as high-power actuators.

Equation 3 showed the inertial velocities in a centrifuge model and the prototype are identical. However, as excess pore pressures are identical at homologous points in model and prototype but the path length is reduced by N, then for the same soil and for the same pore fluid, seepage velocities are increased N times. The high pore pressures in Fig. 2 dissipated according to the differential equation $\partial^2 u/\partial z^2 \alpha \partial u/\partial t$, so that in 1/N scale models they dissipated N^2 times more rapidly than in the prototype. The time for shaking is reduced by N, so to observe excess pore pressures and partial liquefaction in models it is often useful to delay dissipation by a further factor N. In the case illustrated in Figs. 1 and 2 the pore fluid used in a 40 g model test was a 40 centistoke silicon oil and in Figs. 7 and 8 the 80g model test used an 80 centistoke silicon oil.

MODELS TESTED ON CENTRIFUGE SHAKING TABLES

Liquefaction of horizontal ground (Ref. 5) Forty eight aluminium rings with a low-friction coating were stacked up to form a circular container of 12 inch diameter and 12 inch height. The container was filled with sand saturated with silicon oil, with miniature pore pressure transducers at various heights as shown in Fig. 4. While in flight on the Cambridge centrifuge the base of the stacked rings was shaken in the same manner as the base of the embankment in Fig. 2. At each point in the upper part of the column the pore pressure rose to a magnitude equal to the local overburden pressure Fig. 5. The rise in pore pressures in successive cycles of shaking is shown in Fig. 6(a), and after three or four cycles there is an upward hydraulic gradient in the upper part of the column equal to the bouyant weight of the soil. The column of sand would have settled at once if it had been dry, but the presence of pore fluid delayed the settlement. The state of liquefaction of the upper column was simply its fluidisation under the transient flow of the fluid that had to escape to permit settlement. As the excess pore pressures dissipated, Fig. 6(b), and the column of fluidised sand settled a solidification front (Ref. 6) rose up to the ground surface.

This experiment led to a simple interpretation of all the phenomena that are called liquefaction. Liquefaction is the behaviour of soil at or near zero effective stress in the presence of a critical hydraulic gradient (Ref. 7). Where horizontal ground has a stiff upper crust over a layer of saturated sand, the phenomenon of liquefaction can involve cracking of the crust with sand boils

resulting from the high hydraulic gradient and with lateral movement of large blocks of crust during the brief period in which they are floating on a fluidised bed.

Quay walls retaining saturated fill Shaking box or shaking table model studies of the effects of earthquakes on retaining structures have been carried out at 1g since the early work of Okabe to establish the magnitude and distribution of dynamic earth pressure with depth. The models were unsuccessful in determining either the total force or the distribution of pressure, suffering from problems of densification and the high dilatancy of moderately loose sands at low stress levels. However, shaking table studies have been valuable in confirming the basic approach of the block-on-a-plane calculation procedure (Ref. 8) as applied to the displacement of gravity block walls (Ref. 9). These experiments and recent centrifuge model tests (Ref. 10) show clearly the sensitivity of the predicted displacement to the value of ϕ' chosen to calculate the threshold acceleration.

In the modelling of quay walls the degradation of stiffness following pore pressure generation affects the stability of the structure more than the onset of liquefaction in the free field. Fig. 7 shows a flexible anchored cantilever wall model which was subjected to a series of earthquakes (Ref. 11) on the Cambridge 4 m radius centrifuge. Figs. 8(a) and (b) show the acceleration input at the base of the model, the response of the wall in bending as recorded by strain gauges at mid-depth, and the tensile force in one of the tie rods, for each of two earthquakes, numbers 3 and 6. Earthquake 6 was approximately twice the strength of shaking of earthquake 3 and liquefaction was observed behind the wall to at least mid-depth. The cyclic bending moments in Fig. 8(b) are of the order of fifteen times greater than in Fig. 8(a) and very cyclical in nature. As in Fig. 2, the phase of the structural response, as measured by the bending moments in the wall, shifts by 180° following the initial cycle of earthquake 6. Pore pressure rise has provoked a deterioration of stiffness of the anchor system, reducing the fundamental frequency towards the dominant 120Hz of the input base shaking. An analysis of this model by energy methods predicted a natural frequency of around 100Hz in a fully softened condition, but up to 560Hz for a rigid anchor system. The change in phase suggests that the model was softened to below the driving earthquake frequency. The build-up of bending strain in the wall, coupled with the reduction of passive resistance around the toe, led to outward movement and heave in front of the wall.

Piles in earthquakes The examples of sand embankments and quay walls have shown the importance of phase in determining structural response to base shaking, with damage primarily due to pore pressure generation. Model tests of piles subjected to earthquakes in both the Cambridge and Caltech centrifuges have demonstrated the degradation of stiffness due to strain softening (Refs. 12, 13). In the free field, the distribution of shear modulus with depth for a granular aggregate is generally assumed to be proportional to the root of the effective confining pressure, p', and to the void ratio (Ref. 14). Recent experiments have confirmed this approach by the measurement of shear wave velocity with depth in a centrifuge model. An array of 'Bender' elements (Ref. 13), were used to generate and detect a shear wave by 'tweaking' a pair of bonded piezoceramic strips with a voltage pulse. Figs. 9 and 10 show the device and sample data of stiffness versus depth in the free field for a pile model test. Although this type of data provides confidence in the free field modulus and its distribution, close in to a pile severe strain softening has been observed in model tests to dramatically alter the pile response.

Fig. 11 shows centrifuge model of a single pile with a pile cap. Data of the maximum bending moments with depth are shown in Fig. 12 and compared with a pseudo-static analysis which incorporates the lateral and rotational inertia of

the pile cap (Ref. 12). Values of moment are normalised by the predicted surface moment, and depth locations are normalised by the predicted critical length l_c following a pseudo-static approach (Ref. 15). Although a linear variation of shear modulus with depth was assumed to make some allowance for high local strain levels this is clearly inadequate to allow for the actual strain softening around the pile cap in the dynamic case. Observed surface moments are generally lower, and significant moments exist to a greater depth than would be the case under static lateral loading.

If the response of the pile models is idealised as a single degree of freedom system, then the amplitude and phase of the pile cap response will depend on whether the dominant shaking frequency is above or below the fundamental frequency of the soil-pile system. Such an interaction problem is more difficult to address in a 1g model than in a centrifuge model. A non-dimensional group which relates structural stiffness to soil stiffness at any point is given by EI/GH^4 where EI is the bending stiffness of a pile, for example, and G is the shear modulus at a depth H.

Whereas a 1/N scale model at N gravities will maintain similarity, a 1g model of a granular soil for which $G \alpha \sqrt{p'}$ will increase this group by a factor of $\sqrt{N}$. At 1g one option is then to reduce the structural stiffness group, EI, by $\sqrt{N}$ to achieve similarity of soil-structure stiffness. This then increases the natural frequency of the model structure by $N^{0.75}$ (rather than by N), bringing the structural natural frequency into line with the soil natural frequency, which is also increased by $N^{0.75}$ for $G \alpha \sqrt{p'}$. Recalling that for similarity of inertial events frequencies should be increased by $\sqrt{N}$ for a 1g model there is a discrepancy in the ratio of driving frequency to natural frequency. This does not invalidate the technique of 1g modelling, but such tests require careful interpretation.

SOIL BEHAVIOUR AND SHAKING TABLE TESTS

The previous sections have outlined some general principles and given some examples of modelling on shaking tables on centrifuges. The preparation of a body of soil and a structure for testing will depend on the purpose of the model test. Where models are made of soils from actual formations relevant to specific design problems, care will be taken to initialise each elementary volume of soil within the body of the model by an appropriate stress path. Where models are tested for the purpose of validation of a general design calculation the choice of soils and of stress paths is more open.

Static geomechanical models of dams and their foundations are prepared for testing in earth's gravity with equivalent materials - plaster instead of rock and microconcrete instead of real concrete. In such models the material strength is reduced by the same scale as the material dimensions. Similarly it has been proposed (Ref. 16) that centrifuge models could be made with soft clay reconstituted at a water content higher than the prototype by an amount that reduces the rapid undrained strength by an appropriate factor. For example if an increase of water content by half the liquid limit reduces the strength by a factor of 10 then a centrifuge model test of a soft clay model at 100g would correspond to a firm clay prototype 1000 times larger. If such soft clay were used in a model test on a normal shaking table the soft clay model could correspond to a firm clay prototype 10 times larger.

It has been proposed (Ref. 17) that normal shaking table tests should use a relatively looser sand body to correspond to a relatively larger prototype body. Relative density is $I_D = (V_{max} - V)/(V_{max} - V_{min})$, where $V = (1+e)$ is the

Specific Volume, V_{max} the Volume at maximum void ratio e_{max} in a quick tilt test and V_{min} the Volume at minimum void ratio in vibratory compaction. The peak strength of sand tan ϕ' depends on the peak dilatancy rate, which depends both on I_D and on the mean effective stress p' in the aggregate of interlocking sand particles. A corrected relative density $I_R = I_D(10-\ln p')$ appears (Ref. 18) to correlate well with tan ϕ' in sand. To obtain similarity in model and prototype $I_{RM} = I_{RP}$, which requires

$$I_{DM}(10-\ln p'/N) = I_{DP}(10-\ln p'), \qquad (4)$$

hence $I_{DP}/I_{DM} = 1 + \ln N/(10-\ln p')$. Fig. 13 plots this relationship for different values of the mean effective stress p', in a prototype layer. For example, consider a normal shaking table test of a soil body with a layer of sand in the model at a relative density $I_{DM}/I_{DP} = 0.6$. If the model layer is at an effective stress p' = 2.5 kPa when tested, at scale N = 40 then the loose sand in the model will strain similarly to more dense sand in a prototype layer at p' = 100 kPa. However, to model a stratum of uniform sand in a prototype at a unique scale it would be necessary to vary the density of the soil in the model with depth. Furthermore, the dissipation of pore fluid during partial liquefaction of such a loose model layer will probably not be similar to the dissipation in the more dense prototype. However this line of development may allow organisations using normal shaking tables to link their tests with centrifuge model tests.

A large investment has been made in normal shaking tables. A comparable investment is about to be made in shaking tables mounted on centrifuges. As the number of geotechnical centrifuges increases there will be an increasing possibility of organisations possessing centrifuge model test equipment, and preparing their own models for use on one or other of the centrifuges that can be made available at the appropriate time. The development of shaking plates that can be fitted in the base of centrifuge model tests containers may allow organisations to acquire centrifuge model shaking table equipment for much less than the cost of a centrifuge. The introduction of modularity and standardisation of centrifuge model test equipment may make it possible for many organisations which use normal shaking tables to benefit from experience of tests on centrifuges.

REFERENCES

1. Lee, F. H., and Schofield, A. N., "Centrifuge modelling of sand embankments and islands in earthquakes", Geotechnique 38, No. 1, 45-58, (1988).
2. Schofield, A. N., "Geotechnical centrifuge modelling in 1988", Proc. Int. Symp. on Scale Modelling J. S. Mechs. Eng., 263-270, Tokyo, (1988).
3. Craig, W. H., James, R. G., and Schofield, A. N. (eds), Centrifuges in Soil Mechanics, Balkema Rotterdam, (1988).
4. Corte, J-F. (ed), Centrifuge 88, Balkema, Rotterdam, (1988).
5. Heidari, M., and James, R. G., "Centrifuge modelling of earthquake-induced liquefaction in a column of sand', Proc. Conf. on Soil Dynamics and Earthquake Eng. 1 Southampton, 271-281, (1982).
6. Scott, R. F. "Solidification and Consolidation of a liquefied sand column", Soils and Foundations ASCE 26 (4), 23-31 (1986).
7. Schofield, A. N., "Dynamic and earthquake geotechnical centrifuge modelling", Proc. Int. Conf. on Recent Advances in Geotech. "Earthquake Eng. and Soil Dynamics, Vol.3, 1081-1100, Univ. of Missouri-Rolla, (1981).
8. Newmark, N. M., "Effect of earthquakes on dams and embankments", Geotechnique 15, No. 2, June, 139-160, (1965).
9. Richards, R. and Elms, D. G., "Seismic behaviour of gravity retaining walls", Proc. ASCE, JGED, 105, GT4, April, 449-464, (1979).

10. Bolton, M. D., and Steedman, R. S., "Modelling the seismic resistance of retaining structures", Proc. XI ICSMFE, San Francisco, August, 1845-1848, (1985).
11. Steedman, R. S. and Zeng, X., "Flexible anchored walls subject to base shaking", Report CUED/D-SOILS/TR217, Cambridge University, (1988).
12. Steedman, R. S., and Maheetharan, A., "Modelling the dynamic response of piles in dry sand", Report CUED/D-SOILS/TR216, Cambridge University, (1988).
13. Finn, W. D. L., and Gohl, W. B., "Centrifuge model studies of piles under simulated earthquake lateral loading", Proc. Spec. Sess. GED, ASCE Conv. Atlantic City, Geotech. Spec. Pub. 11, 21-39, (1987).
14. Hardin, B. O., and Black, W. L., "Vibration modulus of normally consolidated clay", Proc. ASCE, 105, EM5, 811-827, (1968).
15. Randolph, M. F., "The response of flexible piles to lateral loading", Geotechnique 31, No. 2, 247-259, (1981).
16. Schofield, A. N., "Cambridge geotechnical centrifuge operations", Geotechnique 30, No. 3, 227-268, (1980).
17. Scott, R. F., Unpublished presentation, Centrifuge 88, Paris, (1988).
18. Bolton, M. D., 'The strength and dilatancy of sands', Geotechnique 36, No. 2, 175-195, (1986).

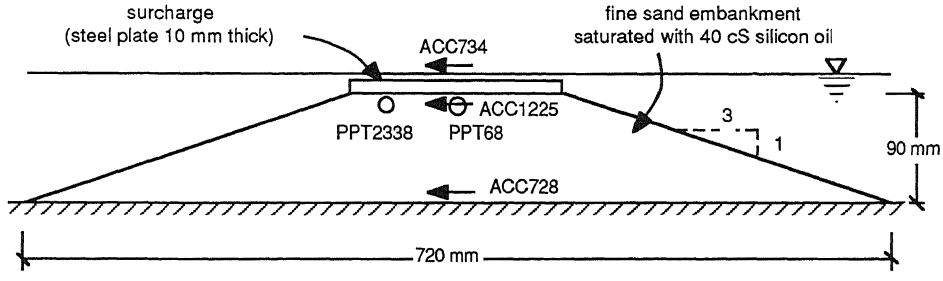

Fig. 1 A model of a saturated soil embankment on a horizontal foundation (after Ref. 1)

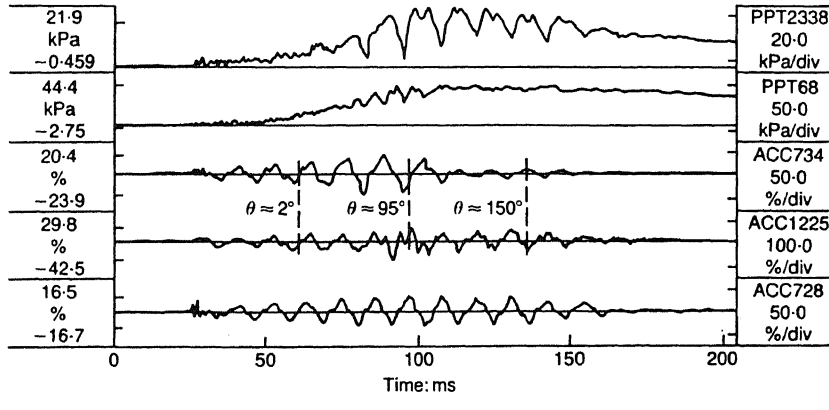

Fig. 2 Acceleration and pore pressure time records from earthquake 7, test FHL01 (after Ref. 1)

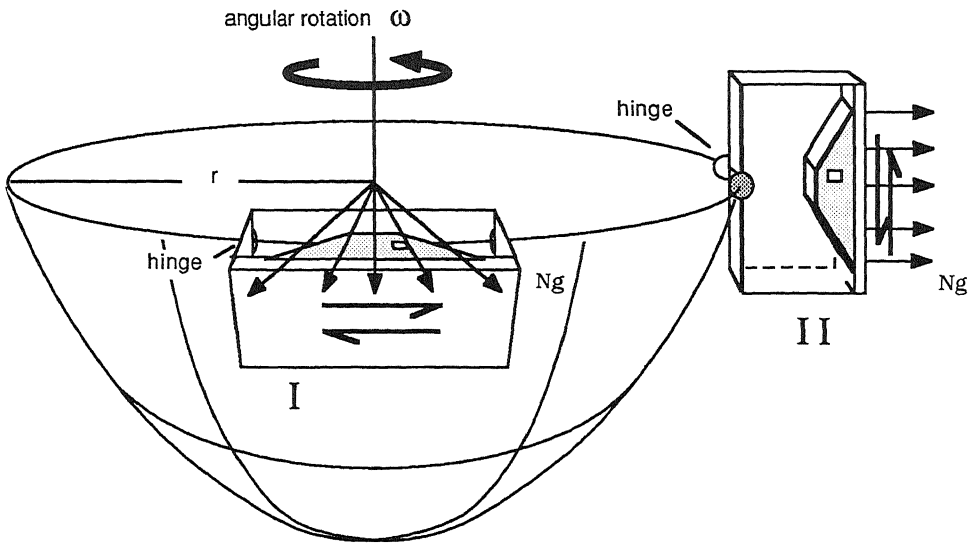

Fig. 3 A paraboloid of revolution about the centrifuge axis

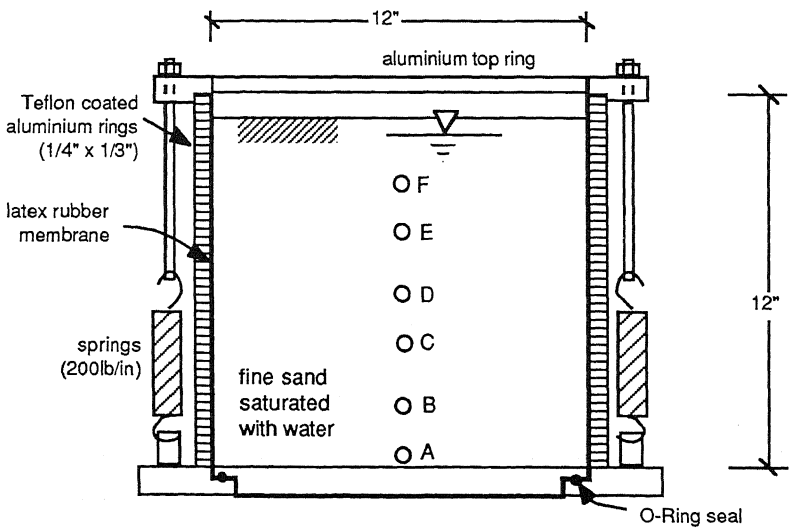

Fig. 4 A 12 inch diameter stacked ring apparatus (Ref. 5)

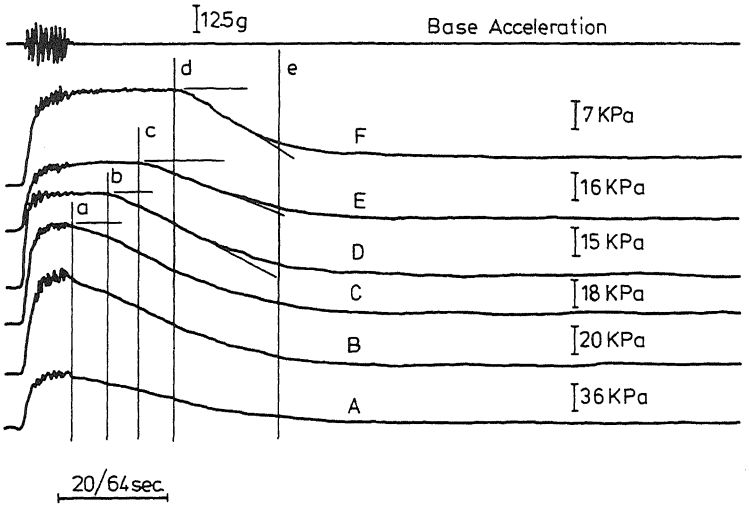

Fig. 5 Excess pore pressure versus time at depths A,B,C,D,E,F (after Ref. 5)

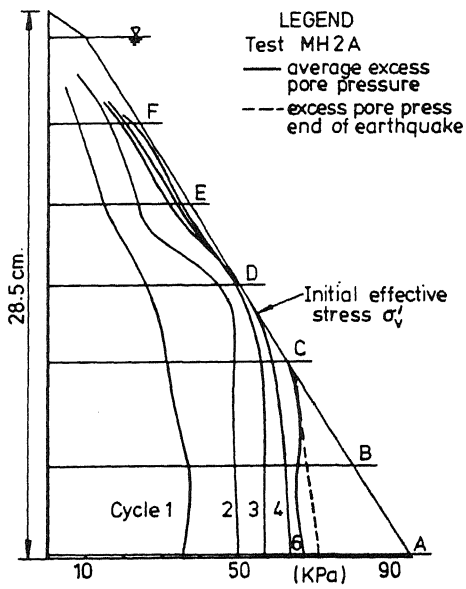

Fig. 6(a) The generation of pore pressure after each cycle of shaking (Ref. 5)

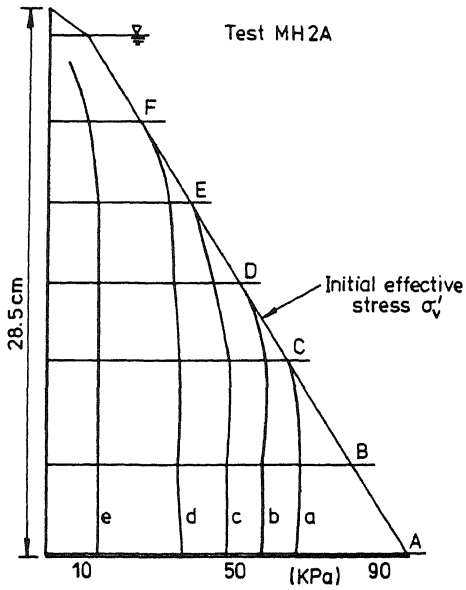

Fig. 6(b) The dissipation of pore pressure at times a, b,c,d,e after the earthquake

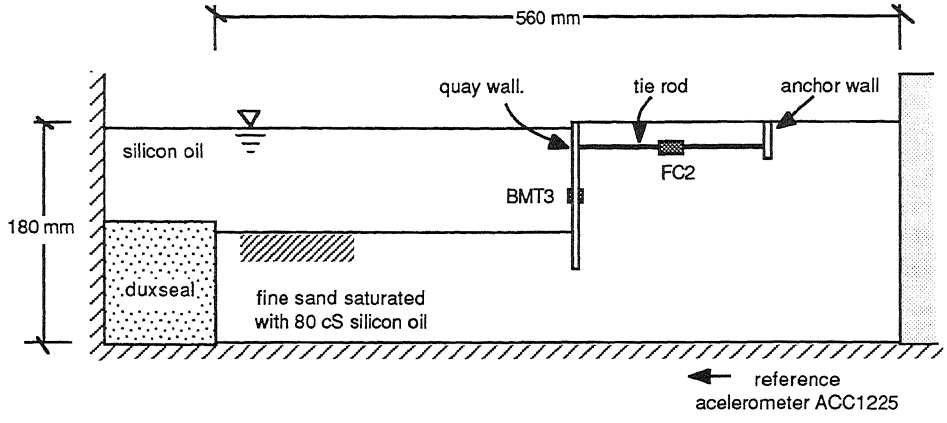

Fig. 7 A centrifuge model at 1/80 scale of an anchored quay wall structure (Ref. 11)

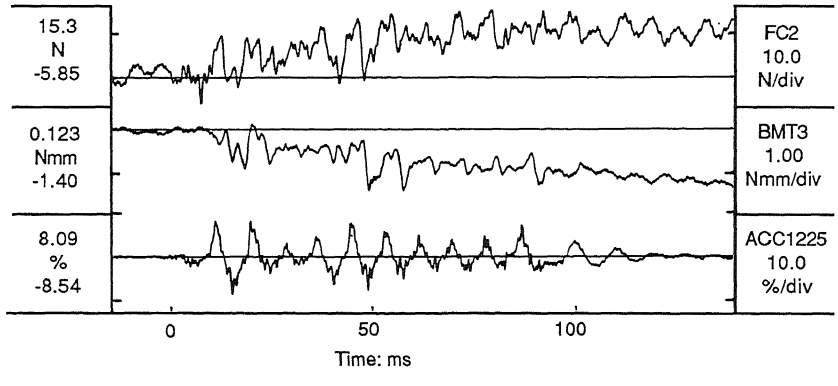

Fig. 8(a) Time records of acceleration, bending moment and anchor force for earthquake 3

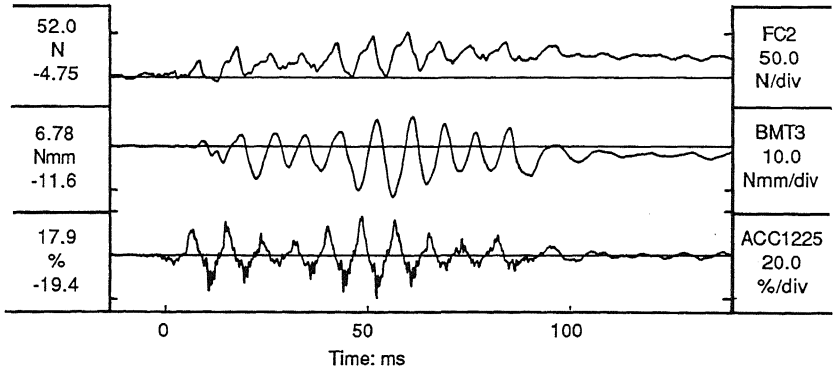

Fig. 8(b) Time records of acceleration, bending moment and anchor force for earthquake 6

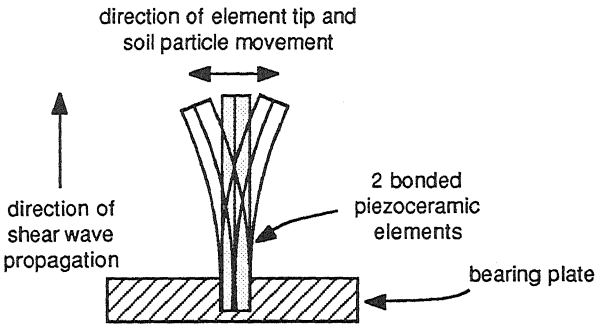

Fig. 9 Vibration of a bender element (after Ref. 13)

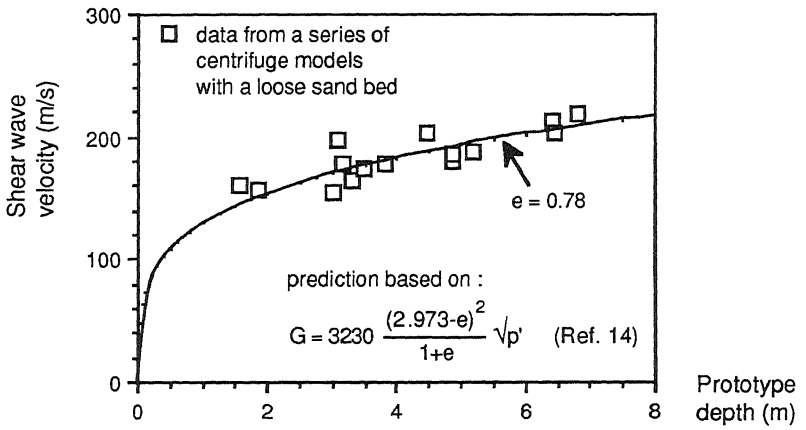

Fig. 10(a) Shear wave velocity measurements (Ref. 13)

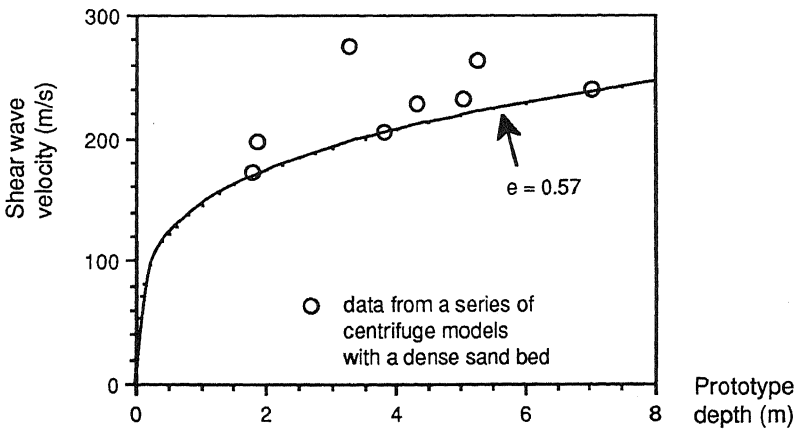

Fig. 10(b) Shear wave velocity measurements (Ref. 13)

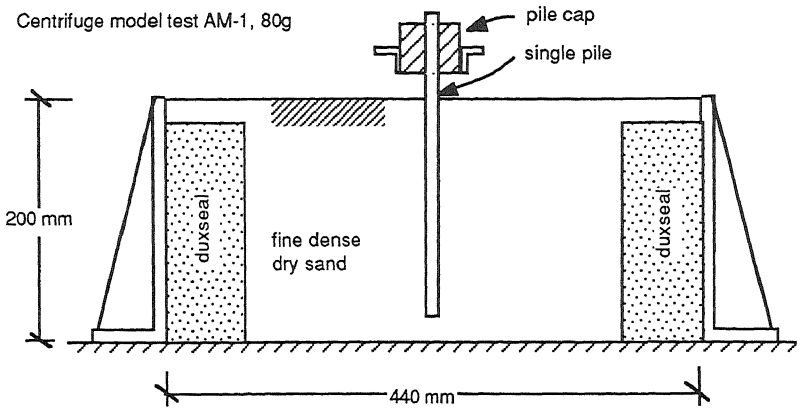

Fig. 11 Centrifuge model test of a single pile (Ref. 12)

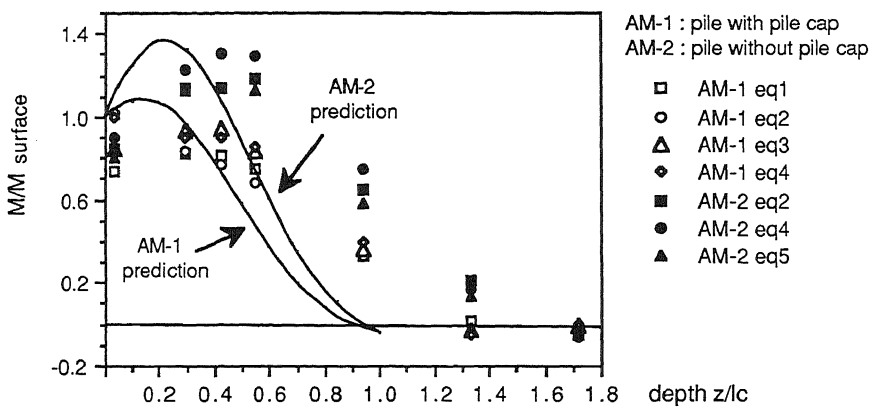

Fig. 12 Data from centrifuge model tests of a single pile

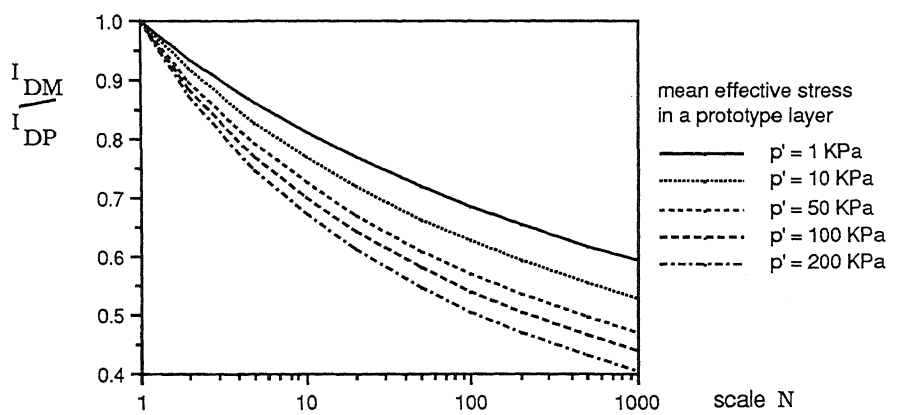

Fig. 13 Relative Density as a function of scale and mean effective stress